PROCEEDINGS OF THE ROYAL SOCIETY A

Proc. R. Soc. A (2008) **464**, 923–942
doi:10.1098/rspa.2007.0221
Published online 17 January 2008

Secondary Turing-type instabilities due to strong spatial resonance

By J. H. P. Dawes* and M. R. E. Proctor

Department of Applied Mathematics and Theoretical Physics, Centre for Mathematical Sciences, University of Cambridge, Wilberforce Road, Cambridge CB3 0WA, UK

We investigate the dynamics of pattern-forming systems in large domains near a codimension-two point corresponding to a 'strong spatial resonance' where competing instabilities with wavenumbers in the ratio 1:2 or 1:3 occur. We supplement the standard amplitude equations for such a mode interaction with Ginzburg–Landau-type modulational terms, appropriate to pattern formation in a large domain. In cases where the coefficients of these new diffusive terms differ substantially from each other, we show that spatially periodic solutions found near onset may be unstable to two long-wavelength modulational instabilities. Moreover, these instabilities generically occur near the codimension-two point only in the 1:2 and 1:3 cases, and not when weaker spatial resonances arise. The first instability is 'amplitude-driven' and is the analogue of the well-known Turing instability of reaction–diffusion systems. The second is a phase instability for which the subsequent nonlinear development is described, at leading order, by the Cahn–Hilliard equation.

The normal forms for strong spatial resonances are also well known to permit uniformly travelling wave solutions. We also show that these travelling waves may be similarly unstable.

Keywords: pattern; symmetry; mode interaction; bifurcation

1. Introduction

Bifurcation theory aims to characterize the possible qualitative changes in the long-time behaviour of a dynamical system as parameters are varied (Guckenheimer & Holmes 1986; Kuznetsov 1997; Wiggins 2003). In recent decades, this has lead to an almost complete theoretical treatment of low-codimension cases; roughly speaking, the codimension of a bifurcation is the typical number of parameters that must be varied in order to explore all different dynamical behaviours that occur nearby.

The systematic study of bifurcation points of higher codimension is important owing to their role as 'organizing centres' for the overall bifurcation structure in a given dynamical system. In the context of pattern-forming instabilities in continuum physical systems, such higher codimension bifurcations are often

* Author for correspondence (j.h.p.dawes@damtp.cam.ac.uk).

Received 21 September 2007
Accepted 14 December 2007

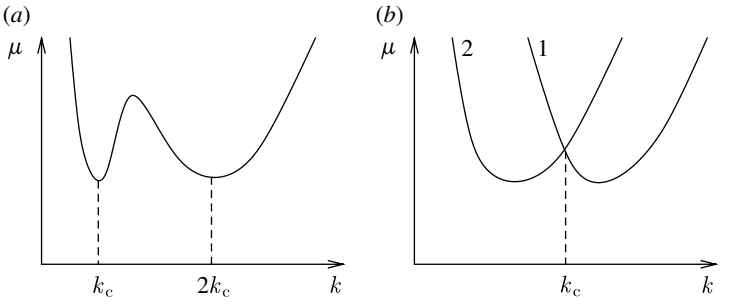

Figure 1. Marginal stability curves in the (k, μ)-plane illustrating the competition between instabilities that leads to a resonant mode interaction. μ denotes a system control parameter. (*a*) The unconstrained case: modes near to k_c and $2k_c$ may generate additional sideband instabilities. (*b*) The constrained case: a mode interaction occurs only in domains of length close to $L=2\pi/k_c$.

referred to as 'mode interactions' (Golubitsky *et al.* 1988; Cross & Hohenberg 1993; Hoyle 2006). Many authors, beginning with Dangelmayr (1986), have investigated the dynamics of a number of such mode interaction problems in spatially extended pattern-forming systems in two or three dimensions, involving various combinations of steady-state and oscillatory instabilities.

In this paper, we return to one of the longest studied of these problems (Dangelmayr 1986; Armbruster *et al.* 1987; Jones & Proctor 1987; Proctor & Jones 1988; Porter & Knobloch 2001) and point out the existence of a new class of instabilities that destabilize spatially periodic 'mixed-mode' equilibrium states in very similar ways to that in which the well-known Turing mechanism destabilizes a spatially homogeneous equilibrium in a pair of coupled reaction–diffusion equations (Murray 2002). We find that the instabilities may be either amplitude-driven or phase-driven, and occur directly as a result of a 'strong spatial resonance' in the mode interaction; they do not occur generically near the mode interaction point in cases of weak, or non-existent, spatial resonance. We consider the 1:2 and 1:3 resonances in detail. The new instabilities, although steady state in nature, are related to the two kinds of oscillatory instability (one leading to travelling waves and another to standing waves) that are present in the normal form ordinary differential equations (ODEs) for these resonant mode interactions. Since neither of these latter instabilities occurs in the weakly resonant or non-resonant cases (i.e. in the simple case of coupled Stuart–Landau equations, where the phases of the modes are not strongly coupled), neither new instability is possible either.

An important distinction in the general set-up of mode interaction problems is between the 'unconstrained' case, where two separate minima in the marginal stability curve for the initial homogeneous state occur for the same value of the control parameter (figure 1*a*), and the 'constrained' case where the smallness of the horizontal domain fixes the wavenumber (figure 1*b*). This paper is concerned with the unconstrained case; we consider a domain that is formally large compared with the pattern wavelength and so may be modulated over large scales. Computations in the constrained case have been carried out by Cox (1996) and Prat *et al.* (2002); although the normal form for the spatial resonance is identical, in this case, the effect of a large horizontal domain would be to allow patterns to evolve into structures on entirely different scales and the mode

interaction at wavenumber k_c would no longer play a central role in organizing the long-time dynamics. However, mode interactions in the unconstrained case arise naturally in many physical problems; for example, the two-layer thermal convection problem discussed in Proctor & Jones (1988) and the multiple instabilities of mushy layers near a solid–liquid interface in solidification problems (see fig. 5 of Worster 1997). The coincidence of the minima of the curves in figure 1*a* at the same value $\mu=\mu_c$ implies that this is a codimension-two bifurcation point. The further requirement that the wavenumber ratio is exactly 1:2 or 1:3 demands, generically, that a third independent parameter must also be varied to observe this bifurcation; a strong spatial resonance is therefore mathematically a codimension-three bifurcation point.

This paper is laid out as follows. In §2 we briefly summarize the computation of the conditions for Turing instabilities in the general case and indicate the relation to spatially uniform oscillatory instabilities; this makes the subsequent presentation entirely self-contained and straightforward. In §3 we discuss the general form of the 'Ginzburg–Landau'-type equations that describe the dynamics at a strong spatial resonance in a large domain, and investigate the two new kinds of instability (referred to as the 'amplitude instability' and the 'phase instability') of the mixed-mode equilibrium. These calculations are illustrated with reference to previous work contained in Proctor & Jones (1988) and Dawes *et al.* (2004). The nonlinear development of the instabilities is examined in §4; for the phase instability, we derive, at leading order, a Cahn–Hilliard equation for the subsequent nonlinear evolution. Numerical simulations confirm the typical dynamics that are expected on theoretical grounds. Section 5 notes the existence of Turing instabilities of uniform travelling wave solutions and §6 concludes.

2. General formulation of Turing instabilities

In this section, we briefly summarize the general theory of Turing instabilities for parabolic partial differential equations (PDEs) of reaction–diffusion type. Consider the pair of scalar PDEs in one spatial dimension,

$$A_t = F(A,B) + \kappa_1 A_{xx} \quad \text{and} \quad B_t = G(A,B) + \kappa_2 B_{xx}, \tag{2.1}$$

where $A(x,t)$ and $B(x,t)$ are suitably smooth real-valued functions defined on the real line $-\infty < x < \infty$, and subscripts denote partial derivatives. The r.h.s. $F(A,B)$ and $G(A,B)$ are typically polynomial functions of their arguments, but it is necessary only that they be sufficiently differentiable for what follows. Naturally, we assume that $\kappa_1, \kappa_2 > 0$. We also suppose that there exists a *uniform* (spatially independent) mixed-mode steady state $A(x,t)=A_0\neq 0$, $B(x,t)=B_0\neq 0$, and we investigate its stability. Let the Jacobian matrix of partial derivatives of F and G, evaluated at (A_0, B_0), be

$$J = \begin{bmatrix} F_1 & F_2 \\ G_1 & G_2 \end{bmatrix}. \tag{2.2}$$

We suppose stability to uniform disturbances, so that

$$F_1 + G_2 < 0 \quad \text{and} \quad \Delta^2 \equiv F_1 G_2 - G_1 F_2 > 0. \tag{2.3}$$

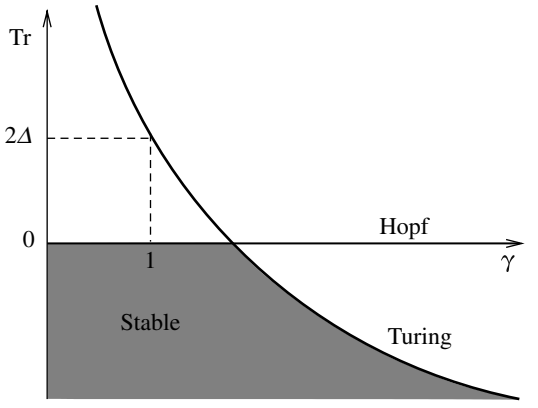

Figure 2. Region of stability of the uniform mixed-mode equilibrium (A_0, B_0) in the (γ,Tr)-plane, for fixed $\Delta>0$ and $F_1<0$. Above the curve marked Turing, the mixed mode is Turing-unstable; above the line marked Hopf, it is unstable to a spatially uniform oscillation.

We look for instability to perturbations proportional to $\cos kx$. The dispersion relation

$$s^2 - s(F_1 + G_2 - (\kappa_1 + \kappa_2)k^2) + \Delta^2 - (\kappa_2 F_1 + \kappa_1 G_2)k^2 + \kappa_1\kappa_2 k^4 = 0$$

shows that instability is possible for wavenumbers k such that

$$\Delta^2 - (\kappa_2 F_1 + \kappa_1 G_2)k^2 + \kappa_1\kappa_2 k^4 < 0,$$

which can be achieved if

$$F_1 + \gamma^2 G_2 > 2\gamma\Delta, \tag{2.4}$$

where $\gamma = \sqrt{\kappa_1/\kappa_2}$. It is clear that the first inequality of (2.3), together with (2.4), can only be simultaneously satisfied if F_1 and G_2 have opposite signs and $\gamma \neq 1$. There are thus two cases,

$$F_1 < 0, \quad G_2 > 0: \quad \text{instability if} \quad \gamma > \frac{1}{G_2}\left(\Delta + \sqrt{\Delta^2 - F_1 G_2}\right) > 1,$$

$$F_1 > 0, \quad G_2 < 0: \quad \text{instability if} \quad \gamma^{-1} > \frac{1}{F_1}\left(\Delta + \sqrt{\Delta^2 - F_1 G_2}\right) > 1.$$

In either case, the critical wavenumber k_{crit} for the onset of the instability, when equality holds in the above expressions, is given by $k_{\mathrm{crit}}^2 = \Delta/\sqrt{\kappa_1\kappa_2}$.

The Turing instability is associated with a (spatially uniform) Hopf bifurcation that occurs when $F_1 + G_2$ changes sign. To understand the relation between them, we fix $\Delta>0$ and $F_1<0$ and plot regions of stability of (A_0, B_0) in the (γ,Tr)-plane, where $\mathrm{Tr} = F_1 + G_2$ (figure 2). For large γ, the Turing instability occurs before the uniform Hopf instability when increasing Tr. For small γ, the reverse is true. The Turing instability is 'associated with' a Hopf instability in the following sense: suppose that the system is at a Hopf bifurcation point, i.e. $F_1 + G_2 = 0$ and $\Delta>0$, and (without loss of generality) suppose that $F_1<0$. Then we see that (2.4) holds for all sufficiently large $\gamma>1$ and hence (A_0, B_0) is Turing-unstable for all sufficiently large γ. Now, for large fixed γ, we

may reduce G_2 (keeping Δ fixed) so that the uniform state (A_0, B_0) is below the Hopf bifurcation line but still above the Turing instability line, i.e. $F_1+G_2<0$ but (2.4) is still satisfied. Hence, just before a Hopf bifurcation from the mixed mode a Turing instability will arise, for γ sufficiently far from unity. The dynamics near the codimension-two point where the Hopf and Turing instabilities occur simultaneously was investigated by De Wit *et al.* (1996).

3. 1:2 and 1:3 resonance with $O(2)$ symmetry

The strong spatial resonances we consider are more completely referred to as $1:n$ resonant steady-state/steady-state mode interactions with $O(2)$ symmetry. The ODE normal form was initially derived by Dangelmayr (1986) and analysed by Armbruster *et al.* (1987) and Jones & Proctor (1987) (for a more general reference containing this material, see Golubitsky *et al.* 1988, ch. XX, section 1). We focus here on the specific cases $n=2$ and 3. In these cases, and in the absence of any additional symmetry restrictions, new coupling terms appear at the second and third order, respectively, in the amplitude equations.

It is the presence of these new coupling terms that allows the much richer bifurcation structure investigated by these earlier authors. When $n=1$, the generic steady-state mode interaction problem is a Takens–Bogdanov bifurcation and has rather different dynamics; we do not consider this case here. We also do not consider the cases of 'weak spatial resonance' corresponding to $n\geq 4$ since the coupling terms appear at order 4 or higher. Since, however, the coupling terms are the only terms that involve the phases of the modes, they are still of great importance, and in order to analyse aspects of the mode interaction dynamics one can justify ignoring 'Landau'-type coupling terms at intermediate orders and including only the resonant coupling terms (e.g. Higuera *et al.* 2004).

In a large domain, it is appropriate to include the effects of modulation of the spatially periodic solutions over long length scales. Our underlying ansatz for instabilities with wavenumbers in the ratio $1:n$, allowing for such spatial modulation, is

$$w(x,t) = \varepsilon\big(A(X,T)\mathrm{e}^{\mathrm{i}x} + B(X,T)\mathrm{e}^{\mathrm{i}nx}\big) + \text{c.c.} + O(\varepsilon^2),$$

where $w(x, t)$ is a variable describing the instability of the initially uniform state. $X=\varepsilon x$ and $T=\varepsilon^2 t$ are the usual scaled length and time variables and $A(X, T)$ and $B(X, T)$ are complex-valued mode amplitudes that, in the absence of spatial resonance, would evolve according to coupled Ginzburg–Landau equations. In the resonant case, the governing amplitude equations, when truncated at the third order, take the form (Dawes *et al.* 2004)

$$\dot{A} = \mu_1 A - A|A|^2 - \lambda_1 A|B|^2 + \alpha_1 B\bar{A}^{\,n-1} + \kappa_1 A_{XX}, \tag{3.1}$$

$$\dot{B} = \mu_2 B - B|B|^2 - \lambda_2 B|A|^2 + \alpha_2 A^n + \kappa_2 B_{XX}, \tag{3.2}$$

where $\mu_{1,2}$ are the bifurcation parameters and $\alpha_{1,2}$, $\lambda_{1,2}$ and $\kappa_{1,2}$ are real coefficients. We assume that the coefficients take generic values and that none vanishes. Solutions of (3.1) and (3.2) with A and B constant correspond to exactly spatially periodic patterns. In the case $n=3$, all the nonlinear terms in (3.1) and (3.2) naturally arise together at the cubic order in the weakly nonlinear theory. In the case $n=2$, the quadratic terms are formally one order in ε larger

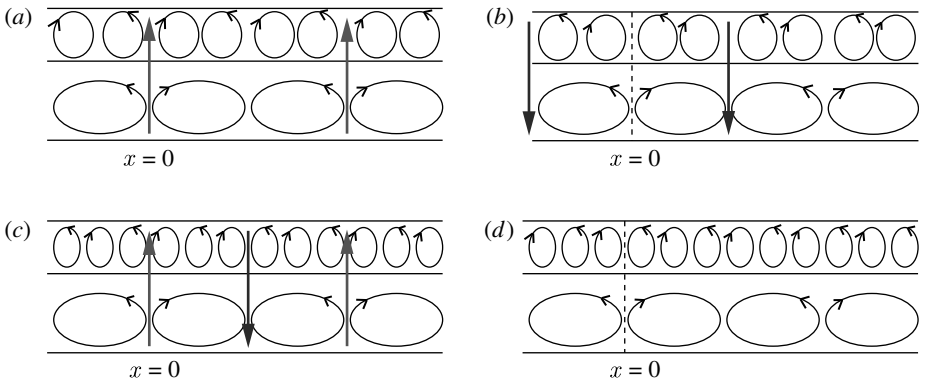

Figure 3. Sketches of the fluid motion for a double-layer Rayleigh–Bénard convection problem, in which the mode Ae^{ix}+c.c. corresponds to convection predominately in the lower layer and the mode Be^{inx}+c.c. corresponds to convection predominately in the upper layer. (*a*) $n=2$, M_+: rising fluid coincides, (*b*) $n=2$, M_-: falling fluid coincides, (*c*) $n=3$, M_+: rising and falling fluid coincides and (*d*) $n=3$, M_-: no coincident rising or falling fluid.

than the cubic terms; to justify this mixing of quadratic and cubic terms, we further assume that the coefficients of the quadratic terms are themselves small, of order ε. This situation would arise if, for example, an additional symmetry that prohibited even-order terms were weakly broken.

To find spatially periodic, uniform amplitude, mixed-mode solutions, we write $A=Re^{i\theta}$ and $B=Se^{i\phi}$ and ignore the spatial derivative terms in (3.1) and (3.2). We obtain

$$\dot{R} = \mu_1 R - R^3 - \lambda_1 RS^2 + \alpha_1 SR^{n-1}\cos\chi, \tag{3.3}$$

$$\dot{S} = \mu_2 S - S^3 - \lambda_2 SR^2 + \alpha_2 R^n \cos\chi, \tag{3.4}$$

$$\dot{\chi} = -\left(n\alpha_1 SR^{n-2} + \alpha_2 R^n S^{-1}\right)\sin\chi, \tag{3.5}$$

where $\chi \equiv \phi - n\theta$ describes the relative phase of the two amplitudes. From (3.5), we see that for mixed-mode equilibria we require $\chi=0$ or π. The mixed-mode amplitudes satisfy

$$0 = \mu_1 R - R^3 - \lambda_1 RS^2 \pm \alpha_1 SR^{n-1},$$

$$0 = \mu_2 S - S^3 - \lambda_2 SR^2 \pm \alpha_2 R^n,$$

where the '$\pm$' are either both '+' ($\chi=0$) or both '−' ($\chi=\pi$). We refer to these solutions as M_+ and M_-, respectively. When $\chi=0$ or π, there is always one mixed-mode equilibrium for which $\theta=0$ and $\phi=0$ or π (respectively), i.e. A_0 and B_0 may both be taken to be real and A_0 may be taken to be positive.

Figure 3 illustrates the mixed modes $M_\pm$ for $n=2$ and 3, in the context of a double-layer convection problem as originally investigated by Proctor & Jones (1988). The flow structures in all four cases are distinct, showing that no two mixed modes are related by symmetry.

To investigate the stability of a mixed mode, we write $A = A_0 + a_1 e^{ikx} + \bar{a}_2 e^{-ikx}$, and similarly for B, and linearize. The 4×4 linear system then isotypically decomposes (using the x-reflection symmetry of the system) into two 2×2 blocks,

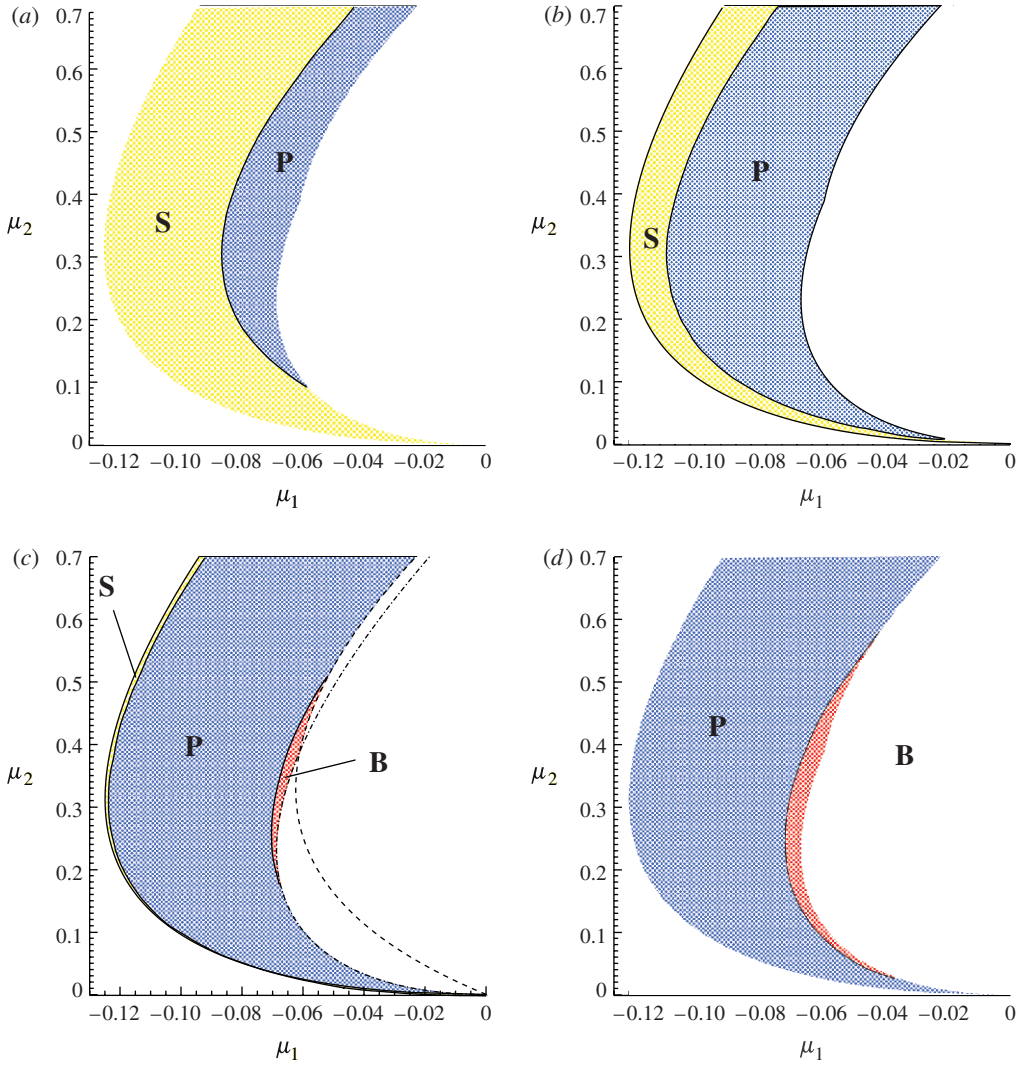

Figure 4. Regions of amplitude and phase instability of M_+ in the (μ_1, μ_2)-plane for $n=2$. Shadings indicate regions of stable existence (S), phase instability (P) and both phase and amplitude instabilities (B). Dashed and dot-dashed lines indicate instabilities of M_+ to travelling and standing waves, respectively. Coefficients are $\lambda_1=2/5$, $\lambda_2=0$, $\alpha_1=1/\sqrt{5}$ and $\alpha_2=-\sqrt{5}$, corresponding to fig. 4 of Proctor & Jones (1988) and fig. 1 of Dawes *et al.* (2004). (*a*) $\gamma=1.5$, (*b*) $\gamma=3$, (*c*) $\gamma=10$: note the slender region of stable M_+ and (*d*) $\gamma=100$.

given conveniently in terms of the variables $P=a_1+a_2$, $Q=b_1+b_2$, $Y=\mathrm{i}(a_1-a_2)$ and $Z=\mathrm{i}(b_1-b_2)$. The factors of i are introduced for consistency with §5. The (P, Q) block is

$$\begin{bmatrix} (n-2)\alpha_1 B_0 A_0^{n-2} - 2A_0^2 - \kappa_1 k^2 & \alpha_1 A_0^{n-1} - 2\lambda_1 A_0 B_0 \\ n\alpha_2 A_0^{n-1} - 2\lambda_2 A_0 B_0 & -2B_0^2 - \alpha_2 A_0^n B_0^{-1} - \kappa_2 k^2 \end{bmatrix}, \tag{3.6}$$

while the (Y, Z) block is

$$\begin{bmatrix} -n\alpha_1 B_0 A_0^{n-2} - \kappa_1 k^2 & \alpha_1 A_0^{n-1} \\ n\alpha_2 A_0^{n-1} & -\alpha_2 A_0^n B_0^{-1} - \kappa_2 k^2 \end{bmatrix}. \tag{3.7}$$

The dynamics described by the P and Q variables concern disturbances to the amplitudes of the modes, while the Y and Z variables describe modulations of their spatial frequencies. We deal with each of these types of disturbance in turn.

(*a*) *Amplitude* (*Turing*) *instability*

The linearization (3.6) fits into the general scheme for Turing instability, discussed in §2, on setting

$$F_1 = (n-2)\alpha_1 B_0 A_0^{n-2} - 2A_0^2, \quad F_2 = \alpha_1 A_0^{n-1} - 2\lambda_1 A_0 B_0,$$
$$G_1 = n\alpha_2 A_0^{n-1} - 2\lambda_2 A_0 B_0, \qquad G_2 = -2B_0^2 - \alpha_2 A_0^n B_0^{-1}.$$

The region of parameter space that is of interest (stability to non-modulated disturbances and potential Turing instability) corresponds to simultaneously satisfying the conditions $F_1 + G_2 < 0$, $F_1 G_2 < 0$ and $F_1 G_2 - F_2 G_1 > 0$. We note that these inequalities cannot be satisfied if $\alpha_1 = \alpha_2 = 0$ and so the resonant coupling terms are essential. For weak resonances ($n \geq 4$), the resonant terms can lead to instability only when the amplitudes are large; in this case, the normal form equations are no longer asymptotically justifiable.

(*b*) *Phase instability*

The second 2×2 block, equation (3.7), corresponds to

$$F_1 = -n\alpha_1 B_0 A_0^{n-2}, \qquad F_2 = \alpha_1 A_0^{n-1}$$
$$G_1 = n\alpha_2 A_0^{n-1}, \qquad G_2 = -\alpha_2 A_0^n B_0^{-1}.$$

This is a degenerate case of the analysis presented in §2 since $\Delta^2 \equiv F_1 G_2 - F_2 G_1 = 0$; the degeneracy arises from the x-translational invariance of the governing equations. The region of interest in parameter space is therefore where $F_1 + G_2 < 0$ (for unmodulated stability) and $F_1 G_2 < 0$ (for potential phase instability). The phase instability is a long-wavelength mode, occurring first at arbitrarily small k, and may occur for α_1 and α_2 arbitrarily close to zero. The pair of inequalities defining the region of interest can be simplified to yield

$$A_0^{n-2} B_0^{-1} \left(n\alpha_1 B_0^2 + \alpha_2 A_0^2\right) > 0, \tag{3.8a}$$

$$\alpha_1 \alpha_2 < 0. \tag{3.8b}$$

For a given value of $\gamma \equiv \sqrt{\kappa_1/\kappa_2}$, we see, from (2.4), that phase instability occurs if $A_0^{n-2} B_0^{-1} (n\alpha_1 B_0^2 + \gamma^2 \alpha_2 A_0^2) < 0$. Subtracting (3.8*a*) from this inequality yields $A_0^n B_0^{-1} (\gamma^2 - 1)\alpha_2 < 0$; for a given γ, this, together with (3.8*b*), indicates the relevant quadrant of the (α_1, α_2)-plane in which instability occurs.

Figures 4 and 5 illustrate these results in the case $n=2$. The coefficients are set to the values used in earlier work, enabling direct comparisons with fig. 4 of Proctor & Jones (1988) and fig. 1 of Dawes *et al.* (2004). We recall from Proctor & Jones (1988) that two mixed-mode equilibria, denoted $M_\pm$, exist in disjoint regions

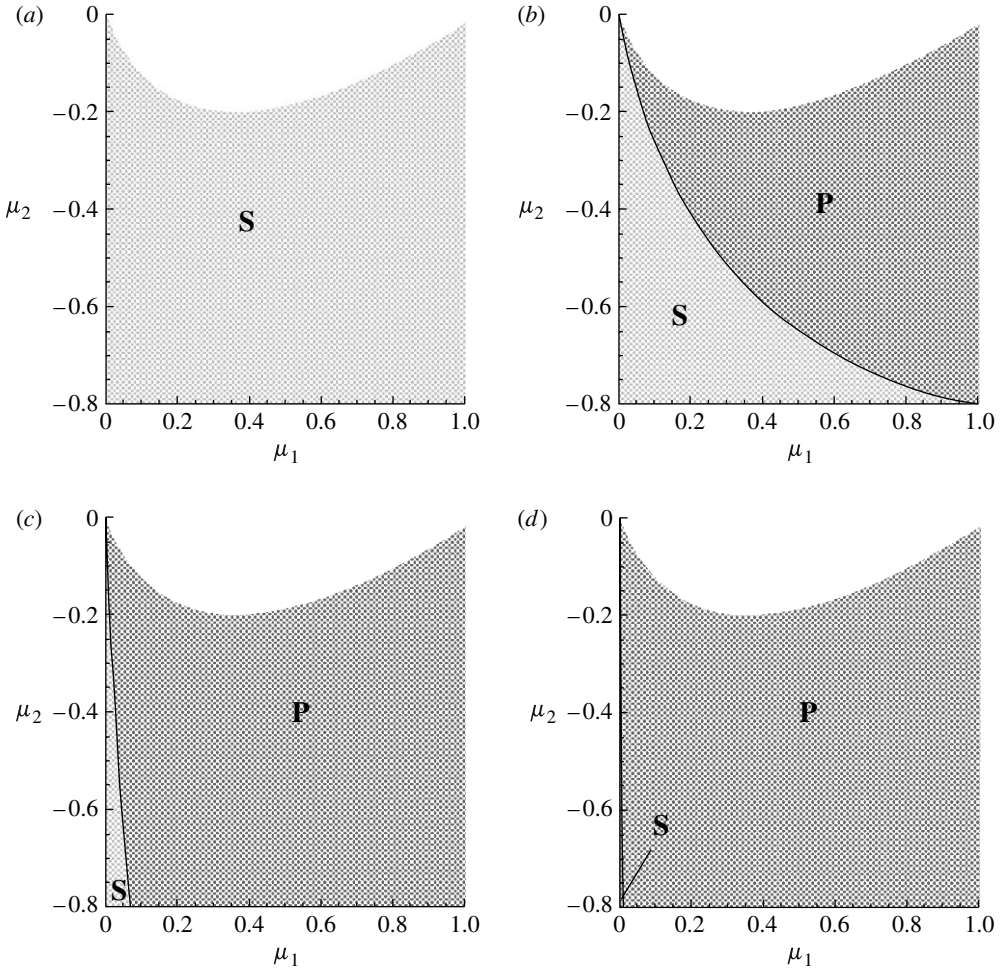

Figure 5. Regions of amplitude and phase instability of M_- in the (μ_1, μ_2)-plane for $n=2$. Shadings indicate regions of stable existence (S) and phase instability (P). Coefficients are $\lambda_1=2/5$, $\lambda_2=0$, $\alpha_1=1/\sqrt{5}$ and $\alpha_2=-\sqrt{5}$, corresponding to fig. 4 of Proctor & Jones (1988) and fig. 7 of Dawes *et al.* (2004). (*a*) $\gamma=3.0$, (*b*) $\gamma=0.7$, (*c*) $\gamma=0.3$ and (*d*) $\gamma=0.1$: note the small region of stable M_- near $(0,-0.8)$.

of parameter space near $\mu_1=\mu_2=0$. For the coefficient values used here, M_+ exist in the quadrant $\mu_1<0$ and $\mu_2>0$, and M_- exist in the quadrant $\mu_1>0$ and $\mu_2<0$. Figure 4 shows that as γ increases, the mixed-mode solution in the quadrant $\mu_1<0$ and $\mu_2>0$ becomes unstable to both amplitude and phase instabilities. The amplitude instability appears in figure 4*c*,*d*; it was not observed for $\gamma=3$. For large γ, the phase instability is found throughout the region where M_+ exist and are stable to non-modulational instabilities.

As we expect from the analysis of §2 and figure 2, with increasing γ the new phase instability appears first near the bifurcation to travelling waves, and the new amplitude instability appears first near the bifurcation to standing waves.

For the two-layer convection problem analysed by Proctor & Jones (1988), we estimate $\gamma\approx 10$ based on the neutral stability curve shown in fig. 2 of that paper; thus, figure 4*c* has a direct physical relevance to this fluid mechanical situation.

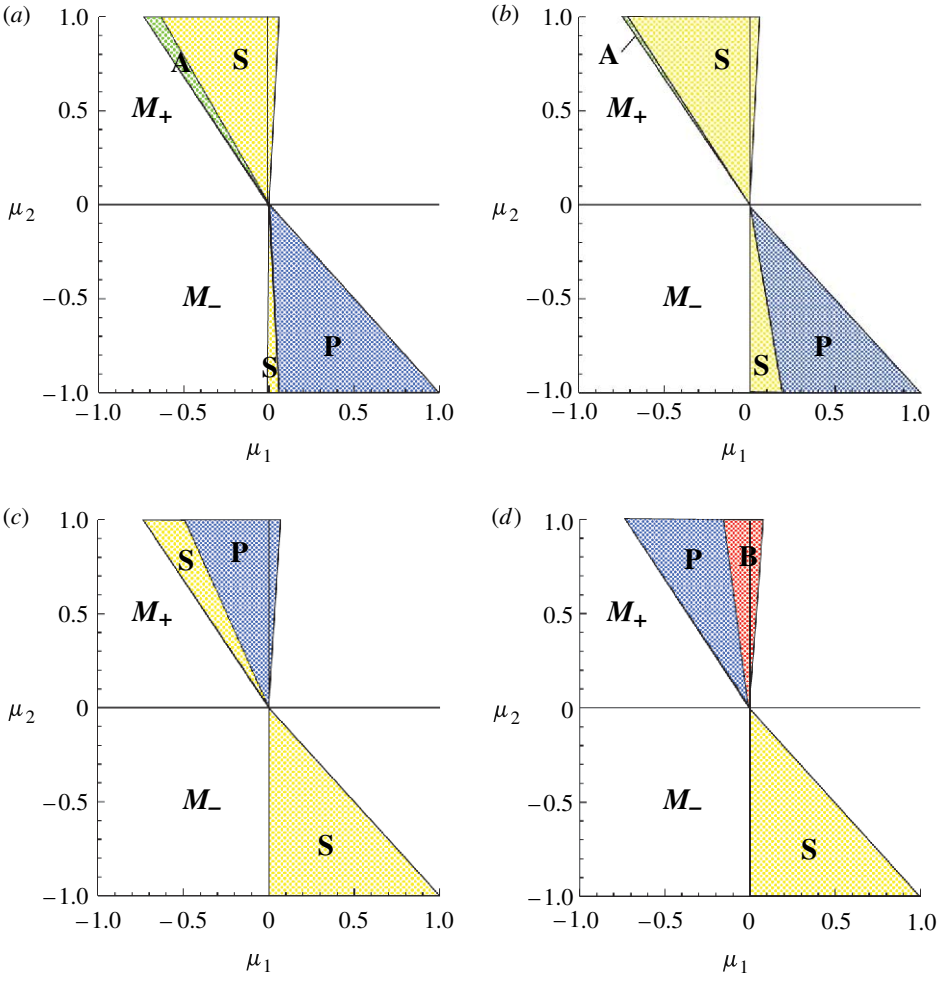

Figure 6. Regions of amplitude and phase instability of the mixed modes $M_{\pm}$ in the (μ_1, μ_2)-plane for $n=3$. For these coefficient values, M_+ exists only in $\mu_2>0$ and M_- exists only in $\mu_2<0$. Shadings indicate regions of stability (S), amplitude instability (A), phase instability (P) and both phase and amplitude instabilities (B). Coefficients are $\lambda_1=\lambda_2=0.3$, $\alpha_1=2.5$ and $\alpha_2=-0.5$. (*a*) $\gamma=0.1$, (*b*) $\gamma=0.3$, (*c*) $\gamma=3$ and (*d*) $\gamma=10$.

Figure 5 shows the onset of phase instability for the M_- equilibrium. We observe that, because $M_{\pm}$ occur in different quadrants, $M_{\pm}$ are phase unstable for opposite signs of γ^2-1 (i.e. M_- are stable for all $\gamma>1$ whereas M_+ are stable for all $\gamma<1$ here).

For the $n=2$ case, it should be noted that many of the complicated features of the bifurcation structure involve secondary codimension-two bifurcation points away from $\mu_1=\mu_2=0$. In any specific physical system, it is therefore not clear how much of the dynamics near these points will actually occur in the dynamics of the original system; only the behaviour near $\mu_1=\mu_2=0$ is guaranteed to relate back to the original underlying system via the weakly nonlinear multiple-scales ansatz outlined at the start of §3.

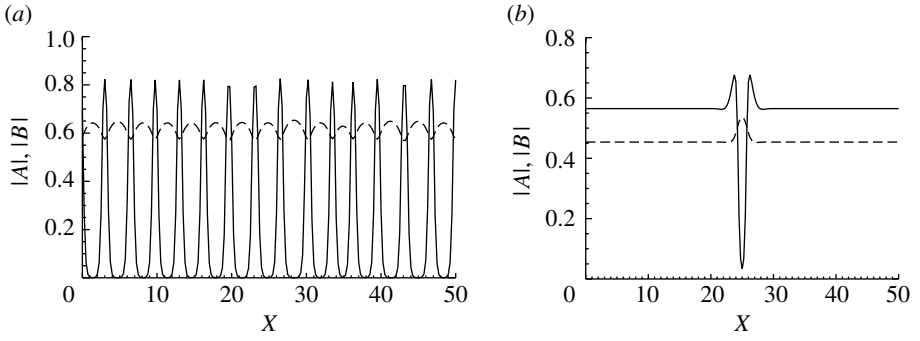

Figure 7. Nonlinear development of the amplitude instability in the case $n=3$, for $\mu_2=0.5$ and $\gamma=0.1$, corresponding to figure 6*a*. For these parameter values, the instability is subcritical. $|A|$ (solid line) and $|B|$ (dashed line). (*a*) Finite-amplitude equilibrium pattern that appears directly after the linear instability of the uniform mixed-mode state for $\mu_1=-0.36$. (*b*) Stable localized modulated state coexisting with the stable mixed-mode state for $\mu=-0.26$. A spatial domain $0\leq X\leq 50$ was used with periodic boundary conditions.

We note that in figure 4*c*,*d*, the phase instability region does indeed extend down to $\mu_1=\mu_2=0$, whereas it does not in figure 4*a*,*b*. Hence, for large enough γ, we anticipate that the phase instability would certainly occur in the original system. Moreover, to examine the genesis of the new instabilities, it is essential to present the bifurcation structure away from $\mu_1=\mu_2=0$. We note that even more complicated dynamics exist in these normal forms further away from the origin (see Porter & Knobloch 2000, 2001).

Figure 6 presents similar illustrative figures for the case $n=3$, again for an indicative collection of parameter values. The presence of only linear and cubic terms in the truncated normal form implies that existence and stability depend only on the ratio μ_2/μ_1 and bifurcations occur only on straight lines. M_+ and M_- exist stably only in the subregions of $\mu_2>0$ and $\mu_2<0$, respectively; the relevant mixed mode is stable in regions labelled S. For $\gamma<1$, there is a slender region of amplitude instability (A) of M_+ in the quadrant $\mu_1<0$ and $\mu_2>0$ (this is only just visible in figure 6*b*), and a much larger region of phase instability (P) of M_- in the quadrant $\mu_1>0$ and $\mu_2<0$. For $\gamma>1$, M_+ in the quadrant $\mu_2>0$ exhibits phase instability, and for $\gamma=10$ (figure 6*d*) there is a subregion (B) of simultaneous instability of M_+. M_- appears to remain stable to the new instabilities when $\gamma>1$.

4. Nonlinear development of the instabilities

(*a*) *Amplitude instability*

The evolution of the instabilities discussed previously for any particular physical problem will naturally depend on nonlinear terms in the perturbation equations. The amplitude instability is of steady-state type, and has an asymptotically small, but non-zero, wavenumber compared with the original periodic pattern. It is therefore a pattern-forming instability of the usual kind for (3.1) and (3.2). Near the instability a universal description is provided by the Swift–Hohenberg equation (Swift & Hohenberg 1977; Iooss & Pérouème 1993;

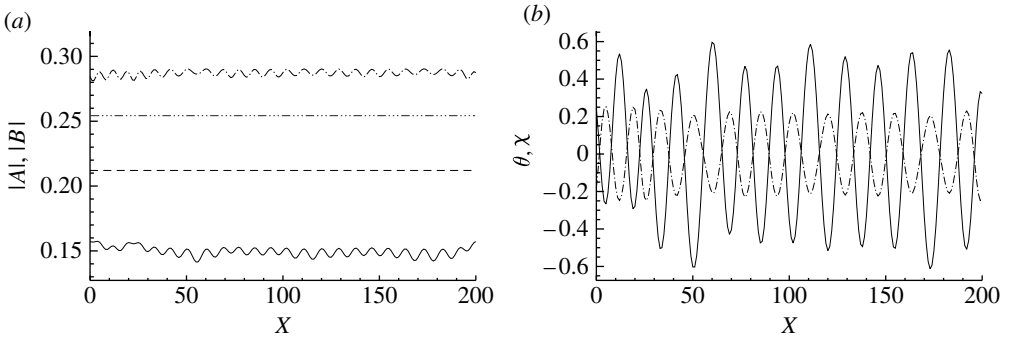

Figure 8. Nonlinear development of the phase instability in the case $n=2$, for $\mu_2=0.5$ and $\gamma=3.0$, corresponding to figure 4*b*. For these parameter values, the instability is supercritical. (*a*) $\mu_1=-0.08$, $|A|$ (solid line) and $|B|$ (dot-dashed line). Horizontal lines indicate the unstable uniform mixed-mode solution at the same parameter values: $|A|$ (dashed line) and $|B|$ (dot-dashed line). (*b*) $\mu_1=-0.08$, θ (solid line) and χ (dashed line). A spatial domain $0 \leq X \leq 200$ was used with periodic boundary conditions.

Hoyle 2006; Pismen 2006) on the long length scales X and T. The instability may be subcritical or supercritical. In the subcritical case (figure 7), we find, as anticipated, both hysteresis and localized states. Alternatively, a further reduction of (3.1) and (3.2), to a Ginzburg–Landau equation involving yet asymptotically longer space and time scales, would be straightforward (but algebraically tedious) in order to determine the subcritical or supercritical nature of the instability. It is interesting to note (from figure 7) the much larger amplitude spatial oscillation in $|A|$ compared with $|B|$, which remains close to its value for the uniform mixed mode. Figure 7*b* shows a localized state that coexists with the uniform mixed mode for $\mu_1=0.5$ and $\mu_2=-0.26$. Such localized states are well known to be generic near a subcritical pattern-forming instability (Sakaguchi & Brand 1996; Coullet *et al.* 2000; Dawes 2007) and the complete bifurcation structure, often referred to as 'homoclinic snaking', is complicated but theoretically well understood (Woods & Champneys 1999; Kozyreff & Chapman 2006). The phases of $A(X, T)$ and $B(X, T)$ remain identically zero for both solutions in figure 7; the instability does not alter the wavelength of the underlying pattern $w(x, t)$, it provides a modulation of only the pattern amplitude.

(*b*) *Phase instability*

The phase instability of the mixed-mode equilibrium occurs in several regions of figures 4–6. In particular, the phase instability occurs for the parameter values corresponding to the two-layer convection problem discussed in Proctor & Jones (1988).

Figures 8 and 9 indicate the nonlinear evolution of the phase instability, in the supercritical case. The final state has an adjusted wavenumber, as indicated by the regular spatial oscillation of the phases θ and χ, and this induces a small spatial variation in the amplitudes $|A|$ and $|B|$ (figure 8*a*). Figure 9 indicates that the initial evolution is towards a state with a shifted wavenumber and new (mean) values of $|A|$ and $|B|$; on a much slower time scale, there is a relaxation towards an exactly spatially periodic structure.

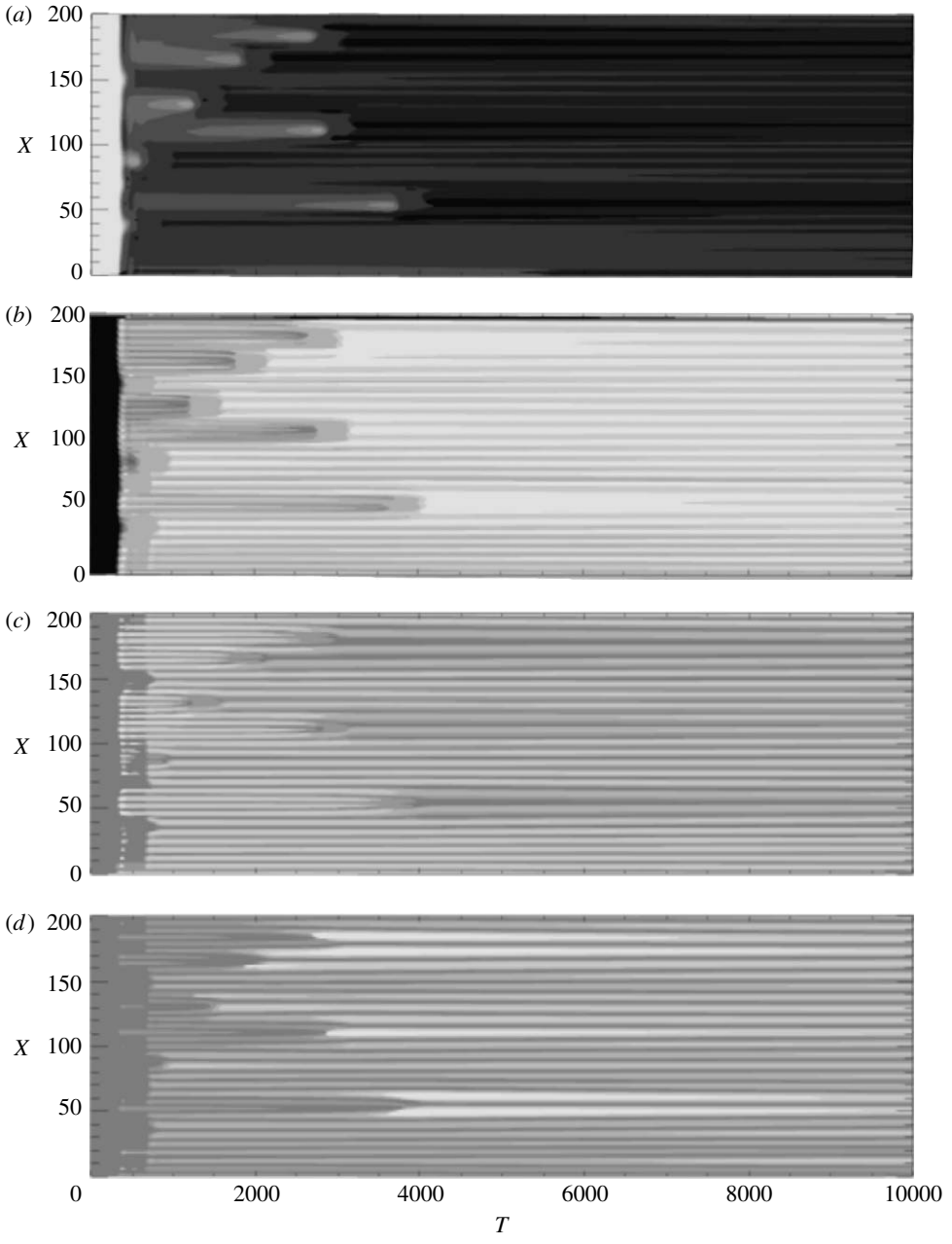

Figure 9. Space–time plots of (*a*) $|A|$, (*b*) $|B|$, (*c*) $\chi \equiv \phi - 2\theta$ and (*d*) θ, showing the nonlinear development of the phase instability of the mixed mode in the case $n=2$, for coefficients λ_1, λ_2, α_1 and α_2 as in figure 4. Parameters are $\mu_1 = -0.08$, $\mu_2 = 0.5$ and $\gamma = 3.0$. A spatial domain $0 \leq X \leq 200$ was used with periodic boundary conditions.

Writing $A(X, T) = R(X, T)\mathrm{e}^{\mathrm{i}\theta(X,T)}$, we anticipate that the weakly nonlinear development of the phase instability can be described by a single equation for the phase $\theta(X, T)$. As usual, we may deduce the general form of the equation by

the application of symmetry arguments; after this brief general discussion, we present the multiple-scales analysis that derives the coefficients in this specific instance.

First, the equation must be of the general form $\dot{\theta} = F(\theta_X, \theta_{XX}, \ldots)$, since neither X nor an undifferentiated θ can appear explicitly due to the translational invariance (and hence the existence of a group orbit of mixed-mode equilibria). The form of the amplitude equations (3.1) and (3.2) implies that the phase equation is equivariant under the two operations $(A, B, X) \to (\bar{A}, \bar{B}, -X)$ and $(A, B, X) \to (A, B, -X)$. The first of these is the usual X-reflection symmetry: in polar coordinates, this operation changes the signs of the phases of A and B. The second operation reflects the fact that the wavenumbers of the instabilities of the basic state are exactly in the ratio $1:n$ and the marginal stability curves of growth rate against wavenumber are parabolic near these wavenumbers. Hence, (3.1) and (3.2) contain only terms with even numbers of X-derivatives. An important consequence of this is that the term $\theta_X\theta_{XX}$ cannot appear and so the resulting phase equation is not of the generic Eckhaus type. Symmetry considerations lead instead to the canonical form

$$\dot{\theta} = -\nu\theta_{XX} - \theta_{XXXX} + \beta\theta_X^2\theta_{XX} + \cdots, \tag{4.1}$$

where ν is the bifurcation parameter, and the sign of β determines whether the bifurcation is supercritical ($\beta>0$) or subcritical ($\beta<0$). Ignoring higher-order terms, (4.1) is the well-known Cahn–Hilliard equation (Novick-Cohen 1998). The sign of β, on which the qualitative dynamics solely depends, may be determined from perturbation theory, as we now discuss. We assume that the parameter values lie on the bifurcation curve for the phase instability. Writing $A = R\mathrm{e}^{\mathrm{i}\theta}$ and $B = S\mathrm{e}^{\mathrm{i}\phi}$, as before, transforms (3.1) and (3.2) into

$$\dot{R} = \mu_1 R - R^3 - \lambda_1 RS^2 + \alpha_1 SR^{n-1}\cos\chi + \kappa_1(R_{XX} - R(\theta_X)^2), \tag{4.2}$$

$$\dot{S} = \mu_2 S - S^3 - \lambda_2 SR^2 + \alpha_2 R^n\cos\chi + \kappa_2(S_{XX} - S(\phi_X)^2), \tag{4.3}$$

$$\dot{\theta} = \alpha_1 SR^{n-2}\sin\chi + \kappa_1 R^{-2}(R^2\theta_X)_X, \tag{4.4}$$

$$\dot{\phi} = -\alpha_2 R^n S^{-1}\sin\chi + \kappa_2 S^{-2}(S^2\phi_X)_X, \tag{4.5}$$

where we have again introduced the phase difference $\chi = \phi - n\theta$. We now introduce a new small parameter ε, and new scaled length and time scales ξ and τ, by writing $\partial_X = \varepsilon\partial_\xi$ and $\partial_T = \varepsilon^4\partial_\tau$. With these scalings, (4.2)–(4.5) become

$$\varepsilon^4 R_\tau = \mu_1 R - R^3 - \lambda_1 S^2 R + \alpha_1 SR^{n-1}\cos\chi + \varepsilon^2\kappa_1(R_{\xi\xi} - R\theta_\xi^2), \tag{4.6}$$

$$\varepsilon^4 S_\tau = \mu_2 S - S^3 - \lambda_2 R^2 S + \alpha_2 R^n\cos\chi + \varepsilon^2\kappa_2(S_{\xi\xi} - S\phi_\xi^2), \tag{4.7}$$

$$\varepsilon^4\theta_\tau = \alpha_1 SR^{n-2}\sin\chi + \varepsilon^2\kappa_1 R^{-2}(R^2\theta_\xi)_\xi, \tag{4.8}$$

$$\varepsilon^4\phi_\tau = -\alpha_2 R^n S^{-1}\sin\chi + \varepsilon^2\kappa_2 S^{-2}(S^2\phi_\xi)_\xi. \tag{4.9}$$

We expand R, S and ϕ in powers of ε^2,

$$(R, S, \phi) = (R_0, S_0, n\theta) + \varepsilon^2(R_2, S_2, \phi_2) + \varepsilon^4(R_4, S_4, \phi_4) + O(\varepsilon^6).$$

At $O(\varepsilon^2)$, the two phase equations yield

$$0 = \alpha_1 S_0 R_0^{n-2}\phi_2 + \kappa_1\theta_{\xi\xi\xi}, \tag{4.10}$$

$$0 = -\alpha_2 R_0^n S_0^{-1}\phi_2 + n\kappa_2\theta_{\xi\xi\xi}. \tag{4.11}$$

These equations are self-consistent provided that $\kappa_1\alpha_2 R_0^2 + n\kappa_2\alpha_1 S_0^2 = 0$, which determines the linear stability boundary. Taking this condition as satisfied, we can now solve for ϕ_2 in terms of $\theta_{\xi\xi\xi}$. Then, turning to the amplitude equations (4.6) and (4.7) at $O(\varepsilon^2)$, we find $R_2 = K_R\theta_\xi^2$ and $S_2 = K_S\theta_\xi^2$, where

$$K_R = \frac{1}{D}\big(-\kappa_1 R_0(2S_0^2 + \alpha_2 R_0^n S_0^{-1}) + n^2\kappa_2 S_0(2\lambda_1 R_0 S_0 - \alpha_1 R_0^{n-1})\big), \tag{4.12}$$

$$K_S = \frac{1}{D}\big(-n^2\kappa_2 S_0(2R_0^2 - (n-2)\alpha_1 S_0 R_0^{n-2}) + \kappa_1 R_0(2\lambda_2 R_0 S_0 - n\alpha_2 R_0^{n-1})\big) \tag{4.13}$$

and

$$\begin{aligned} D = {} & (2R_0^2 - (n-2)\alpha_1 S_0 R_0^{n-2})(2S_0^2 + \alpha_2 R_0^n S_0^{-1}) \\ & - (2\lambda_1 R_0 S_0 - \alpha_1 R_0^{n-1})(2\lambda_2 R_0 S_0 - n\alpha_2 R_0^{n-1}). \end{aligned} \tag{4.14}$$

Making these substitutions in the phase equations (4.4) and (4.5), at $O(\varepsilon^4)$ we obtain

$$\theta_\tau = \alpha_1 S_0 R_0^{n-2}\phi_4 - \kappa_1(S_0^{-1}K_S + (n-2)R_0^{-1}K_R - 4R_0^{-1}K_R)\theta_\xi^2\theta_{\xi\xi\xi}, \tag{4.15}$$

$$\begin{aligned} n\theta_\tau = {} & -\alpha_2 R_0^n S_0^{-1}\phi_4 - n\kappa_2\big(nR_0^{-1}K_R - S_0^{-1}K_S - 4S_0^{-1}K_S\big)\theta_\xi^2\theta_{\xi\xi\xi} \\ & - \frac{\kappa_2\kappa_1}{\alpha_1 S_0 R_0^{n-2}}\theta_{\xi\xi\xi\xi\xi}. \end{aligned} \tag{4.16}$$

Eliminating ϕ_4 between these two results in the Cahn–Hilliard equation

$$c_1\theta_\tau = -\nu\theta_{\xi\xi} + \beta\theta_\xi^2\theta_{\xi\xi} - \kappa_2\kappa_1\theta_{\xi\xi\xi\xi\xi}, \tag{4.17}$$

where

$$c_1 = \alpha_2 R_0^n/S_0 + n\alpha_1 S_0 R_0^{n-2},$$

$$\beta = 6\alpha_2\kappa_1 R_0^n(R_0^{-1}S_0^{-1}K_R - S_0^{-2}K_S).$$

Note that the coefficient $c_1 > 0$ by our assumption of stability to non-modulated perturbations: $F_1 + G_2 < 0$. The coefficient β of the nonlinear term in (4.17) can take either sign, depending on the parameters, and no simple characterization of the stable region appears possible. The linear term in ν is not calculated here: it is linearly related to the (small) distance from the instability boundary; $\nu > 0$ corresponds to the region where the uniform mixed-mode solution is linearly unstable.

Figure 9 shows space–time contour plots of the evolution of the phase instability, for parameter values in the phase unstable region P of figure 4*b*. In this case, we have confirmed analytically that the nonlinear term is stabilizing. It is clear that the amplitudes $|A|$ and $|B|$ adjust quickly and then become slaved to the phases that evolve on a longer time scale.

5. Turing-type instability of travelling waves

In this section, we discuss the existence of a similar instability of uniform travelling wave solutions to (3.1) and (3.2) in the case $n=2$. A uniform travelling wave solution is an X-independent solution, with $\chi = \text{const.} \neq 0, \pi$. From (3.5), we observe that, for uniform states,

$$\dot{\chi} = -\left(2\alpha_1 S + \alpha_2 R^2 S^{-1}\right)\sin\chi$$

and hence for a travelling wave we deduce the constraint $2\alpha_1 S^2 + \alpha_2 R^2 = 0$. The values of R, S and χ are now determined by finding an equilibrium solution to (3.3) and (3.4) that in addition satisfies the constraint.

It is well known that the travelling wave solution undergoes a Hopf bifurcation to so-called 'modulated waves'. In the case $n=2$, this is discussed by Proctor & Jones (1988) (see their eqn (5.15) and the curve Γ in their figures 4 and 5). In the case $n=3$, Porter & Knobloch (2000) note the existence of travelling waves and give a similar condition for the Hopf bifurcation to modulated waves (which they refer to as 'modulated travelling waves'). This instability, together with the analysis in §2, indicates that it is highly probable that travelling waves may also undergo Turing-type instabilities if γ is sufficiently far from unity. It is straightforward to extend the analysis to this case, although, since the Jacobian matrix does not isotypically decompose into 2×2 blocks, analytic criteria for instability are substantially more complicated to obtain than for the mixed modes discussed above. In this section, we set out the Jacobian matrix for reference and present numerical results (figure 10). As expected, for sufficiently large γ, travelling waves are found to be unstable near where they bifurcate from Turing-unstable mixed modes (figure 10*c*,*d*) and near the Hopf bifurcation to modulated waves (figure 10*d*).

Uniform travelling waves take the form $A = R_0 \mathrm{e}^{\mathrm{i}\omega T}$ and $B = S_0 \exp(\mathrm{i}(n\omega T + \chi_0))$, where R_0 and S_0 satisfy (4.2) and (4.3), respectively, after fixing the relative phase $\chi \equiv \phi - n\theta$ to take the value $\chi = \chi_0 \neq 0, \pi$. The evolution equation for χ (combining (4.4) and (4.5)) takes the form

$$\begin{aligned}\dot{\chi} = &-(n\alpha_1 S R^{n-2} + \alpha_2 R^n S^{-1})\sin\chi + n(\kappa_2 - \kappa_1)\theta_{XX} + \kappa_2\chi_{XX} \\ &+ 2\kappa_2 S^{-1} S_X(\chi_X + n\theta_X) - 2n\kappa_1 R^{-1} R_X \theta_X, \end{aligned} \tag{5.1}$$

which implies that $n\alpha_1 S^2 + \alpha_2 R^2 = 0$ is a necessary condition for the existence of travelling waves. We define the frequency $\omega = \alpha_1 S R^{n-2} \sin\chi_0$; the individual phases θ and ϕ evolve according to $n\dot{\theta} = \dot{\phi} = n\omega$.

To examine the stability of the travelling wave state, we write $A = R_0 \mathrm{e}^{\mathrm{i}\omega T} + a_1 \mathrm{e}^{\mathrm{i}kX} + \bar{a}_2 \mathrm{e}^{-\mathrm{i}kX}$ and $B = S_0 \exp(\mathrm{i}(n\omega T + \chi_0)) + b_1 \mathrm{e}^{\mathrm{i}kX} + \bar{b}_2 \mathrm{e}^{-\mathrm{i}kX}$ in the usual way. After substitution and linearization in the (complex) amplitudes a_1, a_2, b_1 and b_2, we form the sum and difference combinations $P = a_1 + a_2$, $Q = b_1 + b_2$, $Y = \mathrm{i}(a_1 - a_2)$ and

$Z=\mathrm{i}(b_1-b_2)$ as before, and derive the 4×4 real Jacobian matrix

$$\begin{bmatrix} -2R_0^2+(n-2)\hat{\omega}-\kappa_1 k^2 & -2\lambda_1 R_0 S_0+\hat{\omega}\dfrac{R_0}{S_0} & -n\omega & \omega\dfrac{R_0}{S_0} \\ n^2\hat{\omega}\dfrac{S_0}{R_0}-2\lambda_2 R_0 S_0 & -2S_0^2+n\hat{\omega}-\kappa_2 k^2 & n^2\omega\dfrac{S_0}{R_0} & -n\omega \\ (2-n)\omega & -\omega\dfrac{R_0}{S_0} & -n\hat{\omega}-\kappa_1 k^2 & \hat{\omega}\dfrac{R_0}{S_0} \\ -n^2\omega\dfrac{S_0}{R_0} & n\omega & -n^2\hat{\omega}\dfrac{S_0}{R_0} & n\hat{\omega}-\kappa_2 k^2 \end{bmatrix},$$

where $\hat{\omega}\equiv\omega\cot\chi_0$. It is easily checked that this matrix has a zero eigenvalue due to the underlying translational symmetry, as discussed earlier.

Figure 10 shows the regions of existence and stability of travelling waves for the same values of λ_1, λ_2, α_1 and α_2 as in figures 4 and 5. The dashed line (on the left-hand boundary of the shaded region) corresponds to the bifurcation from the mixed-mode equilibrium in which travelling waves are created. For $\gamma=1$ (figure 10*b*), where no instability is possible, we find that travelling waves exist stably in two disjoint regions (S) above and below a region where they are unstable to modulated waves, as found by Proctor & Jones (1988). For γ sufficiently far from unity, travelling waves in both regions may become unstable, in the quadrants where mixed-mode equilibria are also destabilized; for $\gamma<1$ (figure 10*a*), we have instability in $\mu_1>0$ and $\mu_2<0$ as in figure 5*d*, and for $\gamma>1$ (figure 10*c*,*d*), we have instability in $\mu_2>0$ as in figure 4*c*,*d*.

From earlier results (Dawes *et al.* 2004, fig. 14), we have observed that, in the case $\gamma=1$, spatio-temporal chaos (STC) coexists the stable travelling waves. A discussion of the (probably spatio-temporally complicated) dynamics resulting from this new instability of travelling waves would therefore have to discern carefully between new STC states arising from unstable travelling waves and those that remain even when $\gamma=1$. We will leave this point for future investigations.

6. Discussion

In this paper we have discussed new instabilities that arise when modulational terms are introduced into the normal forms for the $1:2$ and $1:3$ spatial resonances. Over long length scales the spatially periodic equilibrium and travelling wave states may be destabilized in ways that cannot occur in the absence of strong spatial resonance, and which arise only when the coefficients of the second derivative terms differ sufficiently from each other. These new Turing-like instabilities are therefore additional and novel features of these codimension-three bifurcation problems.

We have shown that mixed-mode equilibria may be unstable separately to either ‘amplitude modes’ or ‘phase modes’ of instability. For travelling waves, it appears that this clear distinction cannot be made, but similar instabilities certainly occur. We remark that the use of asymptotic analysis and Ginzburg–

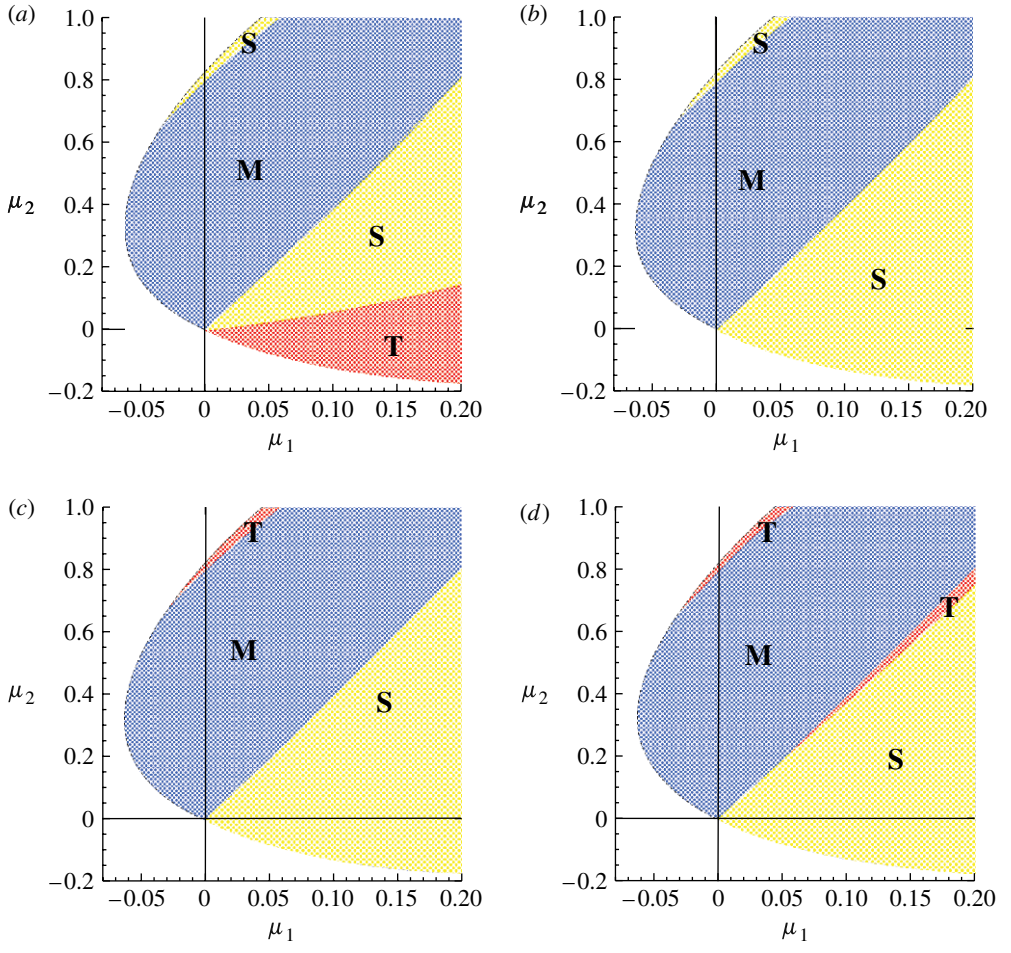

Figure 10. Regions of existence and stability of travelling waves in the (μ_1, μ_2)-plane, for $n=2$. Stable travelling waves (S); TW unstable to modulated waves (M); TW stable to modulated waves but Turing-unstable (T). Coefficients are $\lambda_1=2/5$, $\lambda_2=0$, $\alpha_1=1/\sqrt{5}$ and $\alpha_2=-\sqrt{5}$, corresponding to fig. 4 of Proctor & Jones (1988) and fig. 1 of Dawes *et al.* (2004). (*a*) $\gamma=0.1$, (*b*) $\gamma=1$, (*c*) $\gamma=10$ and (*d*) $\gamma=100$.

Landau-type modelling loses some fine detail that would arise in experimental work, or in direct numerical simulations, for example the locking of fronts to the phase of the underlying periodic pattern.

Also, we have shown that, as is well known in problems of this type, the occurrence of Turing instabilities is linked to the existence of spatially uniform oscillatory instabilities. For the mixed-mode equilibrium, the corresponding spatially uniform instability is the generation of standing wave amplitude oscillations. For the travelling waves, the Turing instability is linked to the generation of spatially uniform so-called modulated waves.

In this paper we have focused on interactions between modes with exactly integer wavenumbers. The amplitude equations (3.1) and (3.2) also admit steady solutions of the form $A(X)=A_0\mathrm{e}^{\mathrm{i}KX}$ and $B(X)=B_0\mathrm{e}^{2\mathrm{i}KX}$; these exist over a similar but shifted region in the (μ_1, μ_2)-plane. We have not considered the

stability of these solutions further, conjecturing that, although additional instabilities (e.g. of Eckhaus type if $|K|$ is sufficiently large) may exist, no qualitatively new features will arise.

Mode interactions do not, however, in general give rise to exact strong spatial resonances; the ratio of wavenumbers need not be close to a ratio of small integers. Such departures from a strong resonance motivated the analysis of Dawes *et al.* (2004) of instabilities generated near to, rather than exactly at, the 1:2 spatial resonance. This earlier paper fixed $\gamma=1$ so as to remove the Turing-type instabilities discussed here, and found that the mixed modes became unstable to modulations (of Eckhaus type) if the frequency mismatch q was sufficiently large. In contrast, in this paper we have shown that there is instability in the exactly 1:2 resonant case ($q=0$) if γ is sufficiently far from unity. Investigating the interactions between these two quite distinct mechanisms for instability will be the subject of a future study. It seems clear on continuity grounds, however, that for wavenumber ratios sufficiently close to 1 : 2, Turing-type bifurcations to modulation should still occur as γ varies away from unity. For example, the interaction of the phase instability governed by equation (4.1) would be modified by the inclusion of a quadratic term of Eckhaus type,

$$\dot{\theta} = -\nu(\gamma, q)\theta_{XX} - \theta_{XXXX} + \delta(q)\theta_X\theta_{XX} + \beta\theta_X^2\theta_{XX},$$

where the coefficient $\delta(q)$ is a function of q, the (scaled) departure, in wavenumber, from exact resonance. The linear stability boundary $\nu=0$ is now, of course, dependent on both q and γ. For sufficiently small $\delta(q)$, corresponding to small deviations from exact resonance, the subcritical or supercritical nature of the phase instability is again determined by the sign of β. We expect the range of parameters over which the instability is supercritical to be reduced since the new term with coefficient $\delta(q)$ serves only to make the bifurcation more subcritical, regardless of the sign of $\delta(q)$ itself.

The authors would like to thank the anonymous referees for their careful reading of the manuscript, and for their comments and suggestions. J.H.P.D. is grateful for financial support from Trinity College and Newnham College, Cambridge, and from the Royal Society through a University Research Fellowship.

References

Armbruster, D., Guckenheimer, J. & Holmes, P. 1987 Heteroclinic cycles and modulated travelling waves in systems with O_2 symmetry. *Physica D* **29**, 257–282. (doi:10.1016/0167-2789(88)90032-2)

Coullet, P., Riera, C. & Tresser, C. 2000 Stable static localized structures in one dimension. *Phys. Rev. Lett.* **84**, 3069–3072. (doi:10.1103/PhysRevLett.84.3069)

Cox, S. M. 1996 Mode interactions in Rayleigh–Bénard convection. *Physica D* **95**, 50–61. (doi:10.1016/0167-2789(96)00041-3)

Cross, M. & Hohenberg, P. C. 1993 Pattern formation outside of equilibrium. *Rev. Mod. Phys.* **65**, 851–1112. (doi:10.1103/RevModPhys.65.851)

Dangelmayr, G. 1986 Steady-state mode interactions in the presence of O_2-symmetry. *Dyn. Stab. Syst.* **1**, 159–185.

Dawes, J. H. P. 2007 Localised convection cells in the presence of a vertical magnetic field. *J. Fluid Mech.* **570**, 385–406. (doi:10.1017/S0022112006002795)

Dawes, J. H. P., Postlethwaite, C. M. & Proctor, M. R. E. 2004 Instabilities induced by a weak breaking of a strong spatial resonance. *Physica D* **191**, 1–30. (doi:10.1016/j.physd.2003.11.009)

De Wit, A., Lima, D., Dewel, G. & Borckmans, P. 1996 Spatiotemporal dynamics near a codimension-two point. *Phys. Rev. E* **54**, 261–271. (doi:10.1103/PhysRevE.54.261)

Golubitsky, M., Stewart, I. N. & Schaeffer, D. G. 1988 *Singularities and groups in bifurcation theory*. Applied mathematical sciences series, vol. 69. Berlin, Germany: Springer.

Guckenheimer, J. & Holmes, P. 1986 *Nonlinear oscillations, dynamical systems, and bifurcations of vector fields*. Applied mathematical sciences series, vol. 42, 2nd edn. Berlin, Germany: Springer.

Higuera, M., Riecke, H. & Silber, M. 2004 Near-resonant, steady mode interaction: periodic, quasi-periodic and localised patterns. *SIAM J. Appl. Dyn. Syst.* **3**, 463–502. (doi:10.1137/030600552)

Hoyle, R. B. 2006 *Pattern formation: an introduction to methods*. Cambridge, UK: Cambridge University Press.

Iooss, G. & Pérouème, M. C. 1993 Periodic homoclinic solutions in reversible 1 : 1 resonance vector fields. *J. Differ. Eqn* **102**, 62–88. (doi:10.1006/jdeq.1993.1022)

Jones, C. A. & Proctor, M. R. E. 1987 Strong spatial resonances and travelling waves in Bénard convection. *Phys. Lett. A* **121**, 224–228. (doi:10.1016/0375-9601(87)90008-9)

Kozyreff, G. & Chapman, S. J. 2006 Asymptotics of large bound states of localized structures. *Phys. Rev. Lett.* **97**, 044502. (doi:10.1103/PhysRevLett.97.044502)

Kuznetsov, Y. A. 1997 *Elements of applied bifurcation theory*. Applied mathematical sciences series, vol. 112, 2nd edn. Berlin, Germany: Springer.

Murray, J. D. 2002 *Mathematical biology*, 3rd edn. Berlin, Germany: Springer.

Novick-Cohen, A. 1998 The Cahn–Hilliard equation: mathematical and modeling perspectives. *Adv. Math. Sci. Appl.* **8**, 965–985.

Pismen, L. M. 2006 *Patterns and interfaces in dissipative dynamics Springer series in synergetics*, vol. XV. Berlin, Germany: Springer.

Porter, J. & Knobloch, E. 2000 Complex dynamics in the 1 : 3 spatial resonance. *Physica D* **143**, 138–168. (doi:10.1016/S0167-2789(00)00099-3)

Porter, J. & Knobloch, E. 2001 New type of complex dynamics in the 1 : 2 spatial resonance. *Physica D* **159**, 125–154. (doi:10.1016/S0167-2789(01)00340-2)

Prat, J., Mercader, I. & Knobloch, E. 2002 The 1 : 2 mode interaction in Rayleigh–Bénard convection with and without Boussinesq symmetry. *Int. J. Bifurc. Chaos* **12**, 281–308. (doi:10.1142/S0218127402004401)

Proctor, M. R. E. & Jones, C. A. 1988 The interaction of two spatially resonant patterns in thermal convection. Part 1. Exact 1 : 2 resonance. *J. Fluid Mech.* **188**, 301–355. (doi:10.1017/S0022112088000746)

Sakaguchi, H. & Brand, H. R. 1996 Stable localized solutions of arbitrary length for the quintic Swift–Hohenberg equation. *Physica D* **97**, 274–285. (doi:10.1016/0167-2789(96)00077-2)

Swift, J. B. & Hohenberg, P. C. 1977 Hydrodynamic fluctuations at the convective instability. *Phys. Rev. A* **15**, 319–328. (doi:10.1103/PhysRevA.15.319)

Wiggins, S. 2003 *Introduction to applied nonlinear dynamical systems and chaos*. Texts in applied mathematics, vol. 2, 2nd edn. Berlin, Germany: Springer.

Woods, P. D. & Champneys, A. R. 1999 Heteroclinic tangles and homoclinic snaking in the unfolding of a degenerate reversible Hamiltonian–Hopf bifurcation. *Physica D* **129**, 147–170. (doi:10.1016/S0167-2789(98)00309-1)

Worster, M. G. 1997 Convection in mushy layers. *Annu. Rev. Fluid Mech.* **29**, 91–122. (doi:10.1146/annurev.fluid.29.1.91)